Clin Exp Nephrol (2015) 19:567–575
DOI 10.1007/s10157-014-1029-3

ORIGINAL ARTICLE

Deficiency of endothelial nitric oxide signaling pathway exacerbates peritoneal fibrosis in mice

Hiroyuki Kadoya · Minoru Satoh · Hajime Nagasu · Tamaki Sasaki · Naoki Kashihara

Received: 23 June 2014 / Accepted: 2 September 2014 / Published online: 13 September 2014

Abstract
Background Long-term peritoneal dialysis (PD) causes peritoneal dysfunction and structural alterations, eventually leading to peritoneal fibrosis. The endothelial nitric oxide synthase (eNOS)–NO signaling pathway contributes to the progression of organ fibrosis. However, it remains unknown whether NO signaling is involved in the process of peritoneal fibrosis. We evaluated the role of the eNOS–NO signaling pathway in the development of peritoneal fibrosis and whether stimulation of soluble guanylate cyclase (sGC), a downstream effector of NO, could attenuate peritoneal fibrosis.
Methods We used wild-type (WT) and eNOS-deficient mice (eNOSKO). The mice underwent mechanical peritoneal stripping-induced peritoneal fibrosis at day 0. At 3, 7, 14, and 28 days after peritoneal stripping, the mice were killed. In some eNOSKO mice, the sGC stimulator Bay 41-2272 was administered by intraperitoneal injection.
Results In WT mice, granulomatous tissue formation was observed in the submesothelial area at days 3 and 7. After day 7, the peritoneal membrane thickness gradually decreased and peritoneal tissue was repaired with leaving only slight fibrosis at day 28. However, eNOSKO mice demonstrated more progression of peritoneal fibrosis than WT mice at 28 days after peritoneal stripping. Expression of vimentin in the thickened peritoneum was prolonged after day 7 in eNOSKO mice. Treatment with Bay 41-2272 significantly attenuated peritoneal vimentin expression and fibrosis in the eNOSKO mice.
Conclusions Disruption of the eNOS–NO signaling pathway exacerbates peritoneal fibrosis by delaying wound healing. sGC stimulation may be a useful therapy for prevention of peritoneal fibrosis.

Keywords Endothelial nitric oxide synthase · Mesenchymal cell · Peritoneal fibrosis · Soluble guanylate cyclase stimulator

H. Kadoya · M. Satoh (✉) · H. Nagasu · T. Sasaki · N. Kashihara
Department of Nephrology and Hypertension, Kawasaki Medical School, Kurashiki, Okayama 701-0192, Japan
e-mail: msatoh@med.kawasaki-m.ac.jp

Introduction

Peritoneal dialysis (PD) is a well-established mode of renal replacement therapy in patients with end-stage renal disease [1, 2]. One of the most important challenges in PD is the long-term preservation of peritoneal membrane integrity. However, long-term exposure to glucose-based PD solution causes peritoneal dysfunction [3]. Prevention of the progression of peritoneal fibrosis is essential for continuation of peritoneal dialysis. However, the detailed mechanisms of the development of peritoneal fibrosis have not been elucidated.

Endothelial dysfunction is characterized by reduced bioactivity of the anti-atherogenic molecule nitric oxide (NO) and is considered a proatherogenic condition [4]. NO, produced by endothelial NO synthase (eNOS), is a biological molecule that mediates the effect of endothelial-derived relaxing factor in blood vessels. The eNOS–NO signaling pathway plays an important role in the process of skin wound healing [5]. It has been reported that a decrease in cutaneous eNOS contributes to impaired wound healing [6]. Moreover, enhancing wound NO bioavailability accelerates diabetic wound healing [7, 8]. Indeed, eNOS–NO is associated with fibrosis in wound-healing processes. Previous data have also suggested that eNOS inhibition

induces and enhances organ fibrosis independently of blood pressure [9, 10]. Although previous reports suggested that chronic PD patients have impaired endothelial function [11], the involvement of eNOS–NO signaling in peritoneal tissue repair and fibrosis is unknown.

Thus, in this study, we hypothesized that disruption of the eNOS–NO signaling pathway in the peritoneal membrane exacerbates peritoneal fibrosis. The aims of this study were to evaluate the role of the eNOS–NO signaling pathway in the development of peritoneal fibrosis using eNOS-deficient (eNOSKO) mice [12] and to investigate the effects of soluble guanylyl cyclase (sGC) stimulation on peritoneal fibrosis.

Materials and methods

Mouse experimental peritoneal injury model

The experimental protocol (No.12-020) was approved in advance by the Ethics Review Committee for Animal Experiments of the Kawasaki Medical School (Kurashiki, Japan) and was conducted according to the Guide for the Care and Use of Laboratory Animals of Kawasaki Medical School based on the National Institutes of Health Guide for the Care and Use of Laboratory Animals (NIH Publications No. 80-23, revised 1996). Wild-type C57Bl/6 J (WT) mice and eNOSKO mice (C57Bl/6 J background) were purchased from Jackson Laboratory (Bar Harbor, ME, USA). Eight-week-old male mice weighting 23–30 g were used in this study. A peritoneal injury model was created by mechanical stripping [13]. At day 0, under sevoflurane inhalational anesthesia, mice were incised at the abdominal midline. The left abdominal wall was opened, and the parietal peritoneal membrane with an area of approximately 1.5 cm^2, including the mesothelial cell monolayer, was peeled off using tweezers and scissors. After the stripping procedure, the abdominal wall was closely sutured. All surgical procedures were performed under sterile conditions. Parietal peritoneal tissues including the wound area were excised under sevoflurane inhalational anesthesia at 3, 7, 14, and 28 days postoperatively ($n = 5$–6 per group for days). Day 0 samples without mechanical stripping were used as a control. The sGC stimulator Bay 41-2272 (Bay; 10 mg/kg/day, Sigma-Aldrich Japan, Tokyo, Japan) was administered postoperatively by intraperitoneal injection once daily for 14 days in some e-NOSKO mice ($n = 6$). These mice were killed and their tissues were examined at 14 days after peritoneal stripping.

Histological and immunohistochemical study

Peritoneal membrane Sects. (4 μm-thick) were prepared from paraffin-embedded tissues and stained with Masson trichrome. For immunohistochemistry, serial sections of paraffin-embedded specimens were rehydrated in phosphate-buffered saline and subjected to microwave antigen retrieval. Antibodies against vimentin (Santa Cruz Biotechnology, Santa Cruz, CA, USA) and cytokeratin 5/8 (BD Biosciences, San Jose, CA, USA) were used as primary antibodies. Negative control studies were performed using irrelevant Ig subclasses similar to those of the primary antibodies, such as nonspecific rabbit IgG or mouse IgG, rather than the primary antibodies. Vimentin was detected using the Histofine Simple Stain MAX-PO (MULTI) kit (Nichirei, Tokyo, Japan) and 3,3-diaminobenzidine (Sigma-Aldrich Japan). In immunofluorescence staining for cytokeratin, tetramethylrhodamine isothiocyanate-labeled anti-mouse IgG (Santa Cruz Biotechnology) was used as a secondary antibody.

Morphological analysis

Masson trichrome-stained specimens and immunohistochemically stained specimens were observed under an inverted microscope (BZ-9000, Keyence, Osaka, Japan). To evaluate the thickness of the wound area in the parietal peritoneum, the distance from the surface mesothelium to the upper limit of the muscular tissue was measured using the measurement module in BZ-H1 M software (Keyence). We measured peritoneal thickness at 10 random points and compared the mean thickness of each tissue. These measurement methods were performed as previously reported [13]. The vimentin-positive area and cytokeratin-covered surface area were also measured using the measurement module in the BZ-H1 M software (Keyence). The vimentin-positive area in the thickened peritoneum was calculated as a percentage and the average area at 10 random points in each tissue was calculated. The area of the cytokeratin-positive cell layer relative to the total peritoneal surface area was calculated as a percentage.

Western immunoblotting

Peritoneal tissue samples were performed using an extraction reagent (T-PER Tissue Protein Extraction Reagent; Thermo Fisher Scientific, Rockford, IL), according to the manufacturer's instructions, and then SDS-PAGE was performed (20 μg protein/lane). Anti-eNOS antibodies were used as the primary antibodies. Signals were detected with the ECL system. Relative optical densities of the bands were quantified with Image J software version 1.42 (http://rsbweb.nih.gov/ij/).

RNA isolation and real-time quantitative PCR

Total RNA was extracted from the anterior abdominal wall using TRIzol (Life Technologies, Grand Island, NY, USA),

followed by digestion with DNase (Sigma-Aldrich Japan). First-strand complementary DNA was synthesized from the total RNA (1 μg) using Moloney murine leukemia virus reverse transcriptase (Life Technologies, Grand Island, NY, USA) with oligo(dT)$_{12–18}$ as a primer [13, 14]. The primers and probes for the TaqMan analysis were designed using sequence information from GenBank using Primer 3 online software (http://frodo.wi.mit.edu/primer3/; accessed January 1, 2014). The primers and probes for α smooth muscle actin (αSMA), collagen, type I, alpha 1 (Col1a1), eNOS, iNOS and nNOS were as follows: αSMA (NM_007392): 5′-caggcattgctgacaggat-3′(forward probe), 5′-gttctggaggggcaatgat-3′ (reverse probe) and 5′-FAM-ctcgcacccagcaccatgaaga-TAMRA-3′ (TaqMan probe). Col1a1 (NM_007742): 5′-tgtgcgatgacgtgcaat-3′ (forward probe), 5′-ttgggtccctcgactcctac-3′ (reverse probe), and 5′-FAM-actggactgtcccaacccccaaag-TAMRA-3′ (TaqMan probe). eNOS (NM_008713): 5′-caggcatcaccaggaagaa-3′(forward probe), 5′-gaatggttgccttcacacg-3′ (reverse probe) and 5′-FAM-atctctgcctcactcatgggcacg-TAMRA-3′ (TaqMan probe). iNOS (NM_010927): 5′-agacctcaacagagccctca-3′(forward probe), 5′-ggctggacttttcactctgc-3′ (reverse probe) and 5′-FAM-ccatgaggctgaaatcccagca-TAMRA-3′ (TaqMan probe). nNOS (NM_008712): 5′-ggcgaacaattccctcatta-3′(forward probe), 5′- ttggaaagaccttgggtcag-3′ (reverse probe) and 5′-FAM- caatgaccgcagctggaagagga-TAMRA-3′ (TaqMan probe). Real-time quantitative PCR was performed using an ABI Prism 7700 sequence detection system (Applied Biosystems, Foster City, CA, USA). The level of expression in each sample was expressed relative to the level of 18S RNA.

Statistical analysis

The values are expressed as the mean ± s. e. m. Parameters were evaluated using a two-tailed unpaired Student's *t* test or one-way analysis of variance for comparison of multiple means. $p < 0.05$ was considered statistically significant.

Results

Peritoneal wound fibrosis in WT and eNOSKO mice after peritoneal stripping

Peritoneal fibrotic changes after a procedure to strip peritoneal mesothelial monolayers were examined in WT and eNOSKO mice. In WT mice, granulomatous tissue formation was observed in the submesothelial area after 7 days (Fig. 1a). The maximum peritoneal membrane

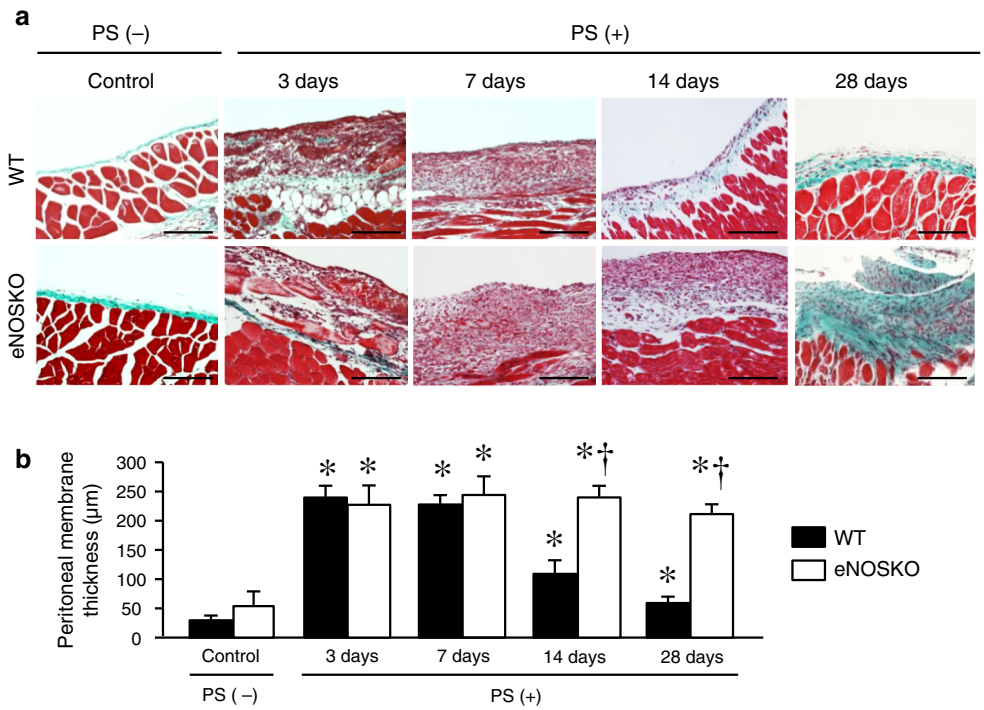

Fig. 1 Pathological changes in the peritoneal membrane after peritoneal stripping (PS). **a** Masson trichrome staining in WT and eNOSKO mice at 3, 7, 14, and 28 days after PS. *Bar* 50 μm. **b** Mean peritoneal membrane thickness of the submesothelial compact zone in WT (*black square*) and eNOSKO mice (*white square*) at 3, 7, 14, and 28 days. $n = 5–6$ for each group. Values are expressed as the mean ± s. e. m. *$p < 0.05$ versus control. †$p < 0.05$ versus WT

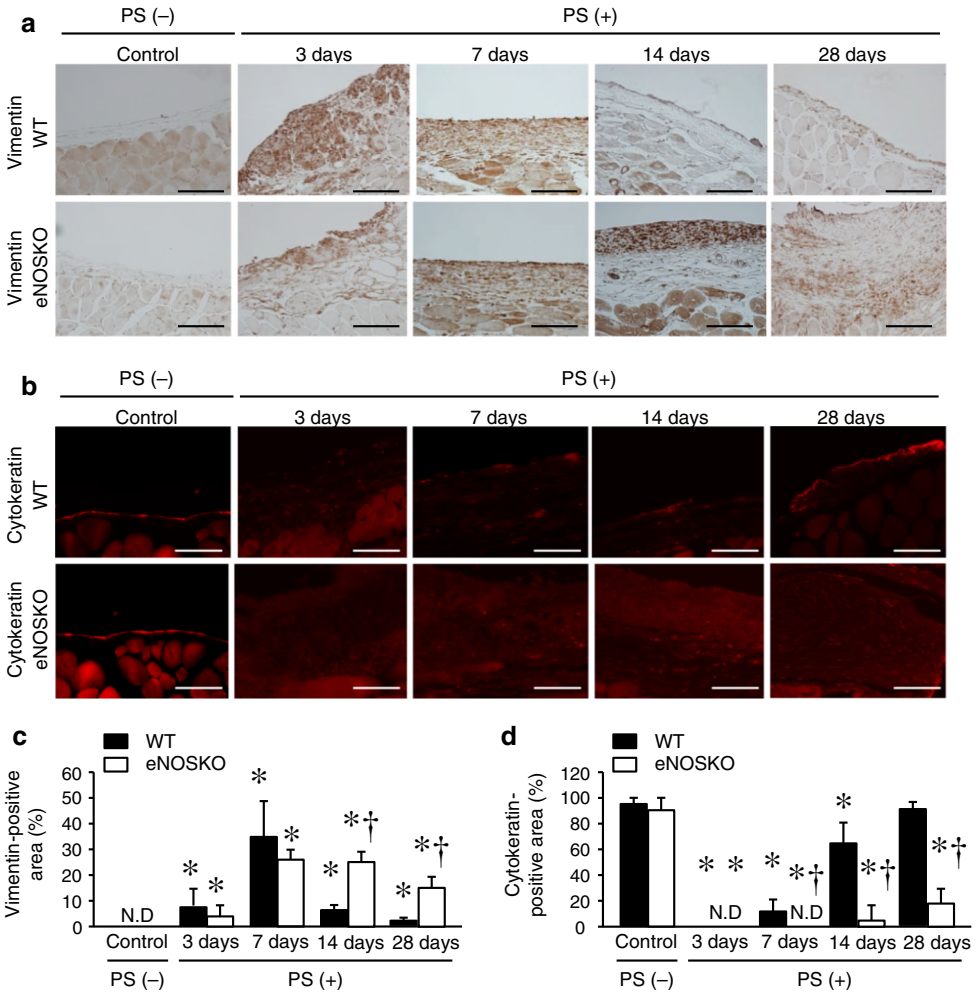

Fig. 2 Expression of vimentin and cytokeratin in the peritoneal membrane after peritoneal stripping. Vimentin (**a**) and cytokeratin (**b**) expression in the peritoneal membrane in WT and eNOSKO mice was evaluated by immunohistochemistry. *Bar* 50 μm. (**c**) Vimentin-positive area in the submesothelial compact zone in WT (*black square*) and eNOSKO mice (*white square*). (**d**) Cytokeratin-positive area in mesothelial cell layer in WT (*black square*) and eNOSKO mice (*white square*). $n = 5$–6 for each group. Values are expressed as the mean ± s. e. m. *$p < 0.05$ versus control. †$p < 0.05$ versus WT

thickness of the submesothelial compact zone was also confirmed at 3 days after peritoneal stripping in WT mice (Fig. 1b). The peritoneal membrane thickness gradually decreased at 14 and 28 days after peritoneal stripping in WT mice. Peritoneal tissue repair was significantly delayed in eNOSKO mice compared with WT mice at 14 days (Fig. 1a, b). Peritoneal thickening by fibrosis was also significantly exacerbated in eNOSKO mice compared with WT mice at 28 days.

Vimentin and cytokeratin expression after peritoneal stripping in WT and eNOSKO mice

The involvement of mesenchymal cell proliferation in the peritoneal wound-healing process was investigated. Vimentin expression after peritoneal stripping is shown in Fig. 2a. The maximum vimentin-positive area in the thickened peritoneum was observed at 7 days after peritoneal stripping in both WT mice and eNOS KO mice. However, the vimentin-positive area in eNOSKO mice was higher than that in WT mice after 14 days (Fig. 2a, c). Next, the involvement of mesothelial cell regeneration in the peritoneal wound-healing process was investigated. Before stripping, a cytokeratin-positive mesothelial cell monolayer was observed on the surface of the peritoneal tissue in WT and eNOSKO mice (Fig. 2b). In both WT and eNOSKO mice, cytokeratin expression disappeared at 3 days. In WT mice, partial regeneration of the cytokeratin-positive cell monolayer was observed at 7 days and the mesothelial cell monolayer had fully recovered at 28 days after peritoneal stripping. (Figure 2b, d). In contrast, cytokeratin expression was not observed in eNOSKO mice until 14 days and the mesothelial cell monolayer had not recovered at 28 days after peritoneal stripping.

Fibrosis-related gene expression after peritoneal stripping in WT and eNOSKO mice

mRNA was extracted from the anterior abdominal wall and gene expression of αSMA (Fig. 3a) and Col1a1 (Fig. 3b) was assessed by real-time quantitative PCR. There were no

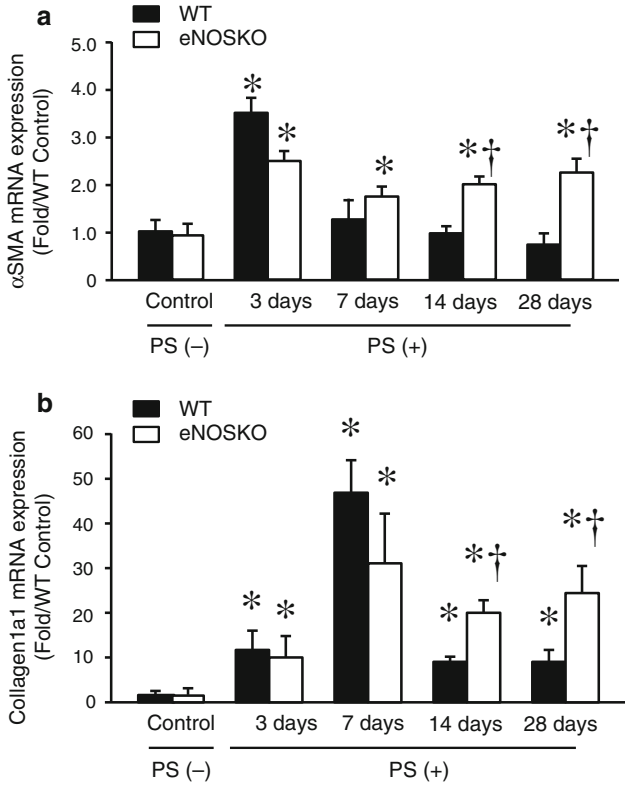

Fig. 3 Evaluation of peritoneal expression of fibrosis-related genes. Levels of mRNA expression for αSMA (**a**) and Col1a1 (**b**) were measured in WT (*black square*) and eNOSKO mice (*white square*) at 3, 7, 14, and 28 days after peritoneal stripping. $n = 5$–6 for each group. Values are expressed as the mean ± s.e.m. $*p < 0.05$ versus control. $\dagger p < 0.05$ versus WT

baseline differences in the expression of both genes between WT and eNOSKO mice. The gene expression data revealed strong upregulation of these fibrosis-related genes in both WT and eNOSKO mice after peritoneal stripping. The maximum levels of αSMA and Col1a1 mRNA expression occurred at 3 and 7 days after peritoneal stripping, respectively (Fig. 3a, b). In WT mice, αSMA and Col1a1 mRNA expression gradually decreased after 14 days, whereas their expression was prolonged in eNOSKO mice compared with WT mice.

Effects of sGC stimulators on peritoneal changes after peritoneal stripping in eNOSKO mice

eNOS–NO signaling after peritoneal stripping was modified by sGC stimulation. There were no changes in the physiological and biochemical parameters in each group except for blood pressure in eNOSKO mice (data not shown). It was shown that Bay did not improve peritoneal thickening at 14 days in WT mice (Fig. 4a, b). However, treatment with the Bay compound markedly ameliorated peritoneal thickening in eNOSKO mice at 14 days (Fig. 4a, b). Vimentin and cytokeratin expression in WT mice was not affected by Bay treatment (Fig. 4a, c, d). On the other hand, expression of vimentin and cytokeratin in eNOSKO mice was ameliorated by Bay treatment. (Figure 4a, c, d). Moreover, αSMA and Col1a1 mRNA expression in eNOSKO mice was improved by Bay treatment (Table 1).

Expression of NOS isoforms after peritoneal stripping in WT and eNOSKO mice

Protein and mRNA were extracted from the anterior abdominal wall. Protein expression of eNOS was assessed by western blotting analysis (Fig. 5a, b). The gene expression of eNOS (Fig. 5c), iNOS (Fig. 5d) and nNOS (Fig. 5e) was assessed by real-time quantitative PCR. Expression of eNOS protein and mRNA levels was increased at 14 days after peritoneal stripping in WT mice. There were no significant differences in the expression of iNOS and nNOS genes between WT and eNOSKO mice. Bay treatment also had no effects on iNOS and nNOS genes expressions (Fig. 5d, e).

Discussion

The aim of this study was to assess the role of the eNOS–NO-sGC signaling pathway in peritoneal fibrosis. Peritoneal tissues of WT mice healed, leaving only slight fibrosis at 28 days after peritoneal stripping. In contrast, peritoneal tissues in eNOSKO mice demonstrated continued mesenchymal cell proliferation, and consequently, fibrosis was increased compared with WT mice. Activation of eNOS–NO signaling by the sGC stimulator attenuated peritoneal fibrosis in eNOSKO mice. The results of the present study suggest that disruption of the eNOS–NO signaling pathway exacerbates peritoneal fibrosis by delaying wound healing and the treatment of sGC stimulation may be a useful therapy for prevention of peritoneal fibrosis.

Three possible mechanisms exist for peritoneal fibrosis progression in eNOSKO mice. First, wnt/beta-catenin signaling plays a pivotal role in interstitial fibrosis in several progressive disease models such as lung and liver fibrosis [15, 16]. Furthermore, it has been reported that the cGMP/protein kinase G (PKG) pathway inhibits tumor cell growth through transcriptional suppression of wnt/beta-catenin [17]. It is also possible that wnt signaling is activated by inhibition of the NO/cGMP/PKG signaling pathway. Second, endothelium-derived NO is a mediator of angiogenesis [18]. Therefore, blood flow reduction resulting from reduced eNOS levels may delay tissue repair. Third, decreased matrix metalloprotease (MMP) activity may have exacerbated peritoneal fibrosis in eNOSKO mice. Several recent studies have suggested that NO is involved

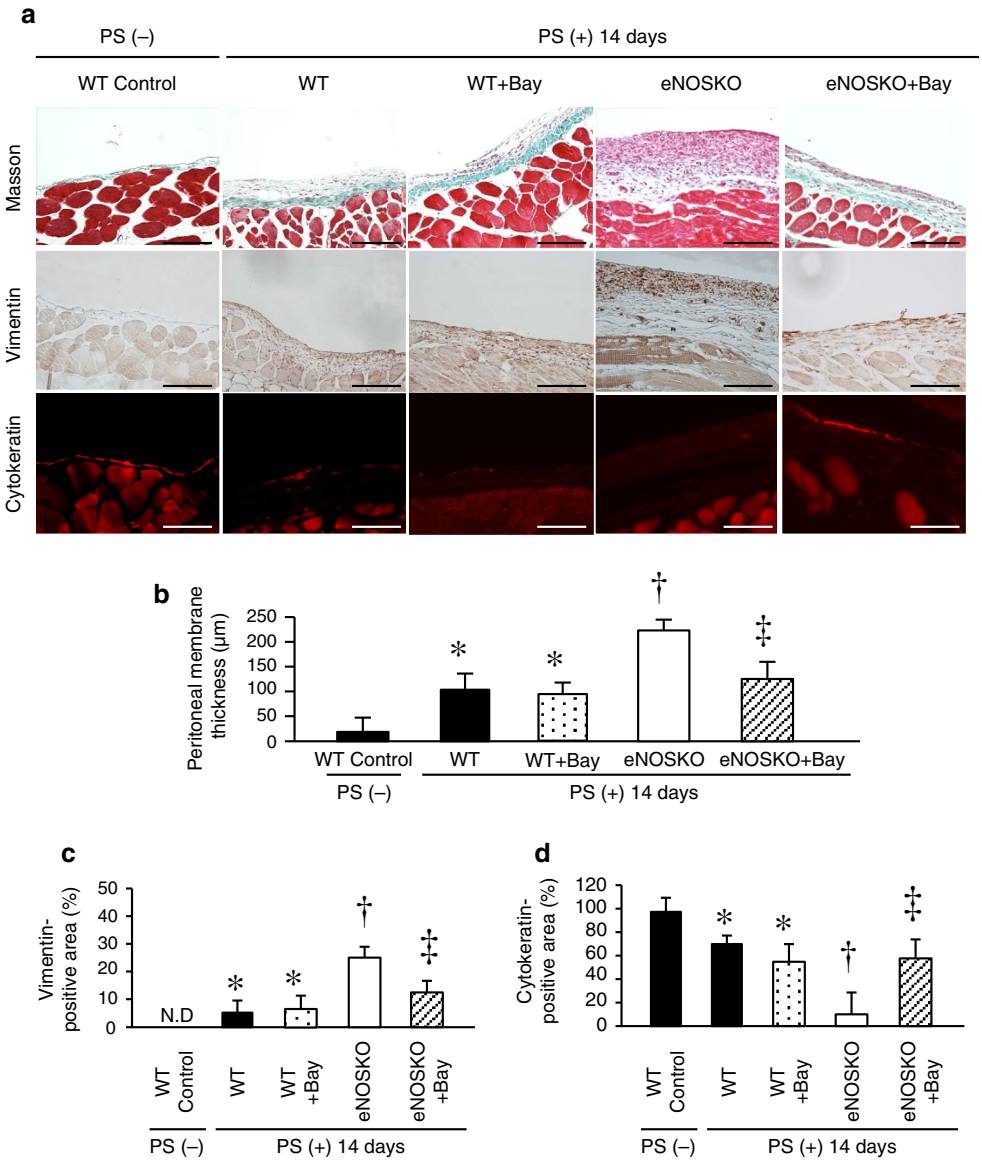

Fig. 4 Fig 4. Effects of an sGC stimulator on peritoneal fibrosis after mechanical stripping in WT and eNOSKO mice. **a** Masson trichrome staining (*upper*), vimentin immunohistochemical staining (*middle*), and cytokeratin immunohistochemical staining (*lower*) of the peritoneal membrane in WT and eNOSKO mice at 14 days after mechanical stripping. In some WT and eNOSKO mice, the Bay 41-2272 compound was administered for 14 days by intraperitoneal injection (WT + Bay, eNOSKO + Bay). *Bar* 50 μm. **b** Mean peritoneal membrane thickness of the submesothelial compact zone. **c** Vimentin-positive area in the submesothelial compact zone. **d** Cytokeratin-positive area in mesothelial cell layer. $n = 5$–6 for each group. Values are expressed as the mean ± s. e. m. *$p < 0.05$ versus WT control. †$p < 0.05$ versus WT. ‡$p < 0.05$ versus eNOSKO

Table 1 Effect of sGC stimulation in eNOSKO mice at 14 days after peritoneal stripping

	WT	eNOSKO	eNOSKO + Bay
αSMA ($\times 10^{-2}$ copy/18S RNA)	0.6 ± 0.1	1.0 ± 0.2 [a]	0.4 ± 0.1[b]
Col1a1 ($\times 10^{-3}$ copy/18S RNA)	1.4 ± 0.3	3.8 ± 1.3[a]	1.1 ± 0.6[b]

WT C57BL/6 J mice; *eNOSKO* endothelial nitric oxide synthase knockout mice; *Bay* Bay 41-2272 treatment. $n = 6$ in each group

[a] $p < 0.05$ versus WT

[b] $p < 0.05$ versus eNOSKO

in the activation of MMPs [19]. Hence, it is necessary to examine the detailed molecular mechanism of peritoneal fibrosis in eNOSKO mice.

We confirmed that peritoneal wound healing was significantly delayed in eNOSKO mice. We also evaluated NOS isoforms at 14 days following mechanical peritoneal stripping. There was no difference in the expression of iNOS and nNOS between WT and eNOSKO mice at 14 days following mechanical peritoneal stripping. In contrast, eNOS expression was significantly increased at 14 days after peritoneal stripping in WT mice. It has been reported that inhibitors of NOS delay the wound-healing process in skin, [20, 21]. In particular, eNOS deficiency has been reported to contribute to impaired wound healing in the skin [6]. There is currently no study that evaluates NOS expression in the peritoneal wound-healing process after mechanical stripping. The same wound-healing process that occurs in the skin may occur in the peritoneal membrane. Our data suggests that eNOS is an important source

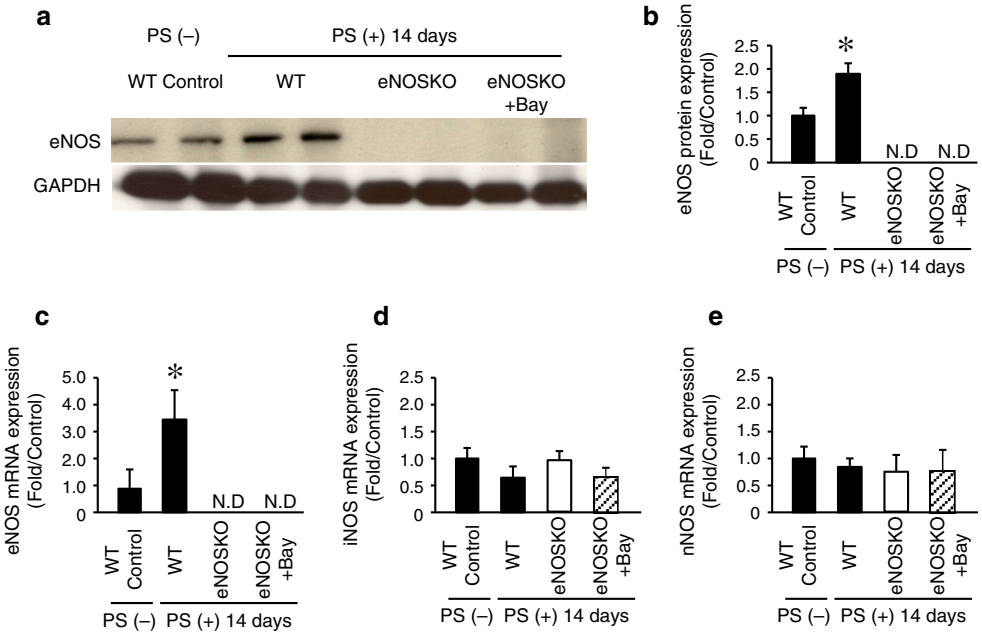

Fig. 5 Expression of NOS isoforms in the peritoneal membrane after peritoneal stripping. Protein expression of eNOS in WT and eNOSKO mice at 14 days after peritoneal stripping (**a**, **b**). Levels of mRNA expression for eNOS (**c**), iNOS (**d**) and nNOS (**e**) were measured in WT and eNOSKO mice at 14 days after peritoneal stripping. $n = 5$–6 for each group. Values are expressed as the mean ± s.e.m. $^{*}p < 0.05$ versus WT control

of NO production in PF after the shedding of peritoneal mesothelial cells by mechanical stripping. The cutaneous wound-healing process is subdivided into three complementary and overlapping phases: inflammation, granulation tissue formation (proliferative), and remodeling [22]. Various factors are involved in wound healing such as cytokines and growth factors, extracellular matrix components, and several cell types [22, 23]. Thais et al. reported that topical application of a NO donor in both the inflammatory and proliferative phases improves rat cutaneous wound repair by accelerating epithelialization [24]. Indeed, NO plays an important role in accelerating the wound-healing process in the inflammatory and proliferative phases. However, peritoneal fibrosis may be exacerbated because of prolonged mesenchymal cell proliferation. We did not evaluate the origin of myofibroblasts in the peritoneal membrane after mechanical stripping in the present study. In the peritoneum, the proportions of myofibroblasts that originate from resident fibroblasts [25], circulating fibrocytes [26], and mesothelial cell [27] remain unclear and should be further evaluated.

Our results indicate that sGC stimulation could restore the impaired peritoneal membrane morphology after mechanical stripping in eNOSKO mice. In contrast, the sGC stimulator had no effect on the peritoneal wound-healing process in WT mice, indicating that the sGC stimulator cannot accelerate the peritoneal wound-healing process under normal conditions in which eNOS-derived NO is supplied. Most NO effects are mediated by activation of sGC, generation of cGMP, and activation of PKG [28]. sGC functions as an NO sensor and it has been shown to promote angiogenesis [29]. It has been reported that an sGC stimulator (iontophoresis) induced a sustained increase in rat skin blood flow [30]. Moreover, Beyer et al. reported that an sGC stimulator (BAY41-2272) stopped the development of bleomycin-induced dermal fibrosis and skin fibrosis in mice [31]. Recently, riociguat, a member of a new class of sGC stimulator compounds, significantly improved exercise capacity and pulmonary vascular resistance in patients with chronic pulmonary hypertension in a randomized, double-blind, placebo-control study [32]. Therefore, we expect that sGC stimulators will have clinical effects against peritoneal fibrosis. Phosphodiesterase inhibitors also activate PKG and may therefore have the same effect as sGC stimulators in peritoneal wound healings.

One limitation of this study is that this model is not entirely suitable as a model of PF. Rather, our experimental model represents the wound-healing process of peritoneal mesothelial cells after mechanical stripping. This is the most obvious limitation of this study. The most commonly used method to create a PF model is an intraperitoneal injection of 0.1 % chlorhexidine gluconate (CG) [33, 34]. It is true that CG-induced peritoneal fibrosis does not fully replicate peritoneal sclerosis or EPS observed in patients on long-term PD. However, there is no ideal experimental model that allows for simulation of long-term PD. Evaluation of another PF model showed that repeated injection of a high-glucose solution may reflect the pathogenesis of peritoneal injury in PD patients [35] in a better way than chlorhexidine gluconate injection. High-glucose concentration, low pH, and the presence of glucose degradation products in PD solutions can also cause changes in peritoneal membrane morphology [36]. Additional studies will

be required to ascertain whether the eNOS–NO signaling pathway may provide protection against the effects of CG in patients with PD dialysate solution-induced long-term peritoneal damage. Activation of the eNOS–NO signaling pathway accelerates angiogenesis. It has been reported that angiogenesis and vessel permeability are key factors in ultrafiltration dysfunction in PD [37, 38]. However, the relationship between fibrosis and angiogenesis has not been clearly defined. Margetts et al. reported that fibrosis and angiogenesis may be two separate responses to peritoneal injury [39]. Future studies should address this point.

In conclusion, this study indicates that dysfunction of the eNOS–NO signaling pathway exacerbates peritoneal fibrosis. Treatment with sGC stimulators may be a novel therapeutic target to attenuate peritoneal fibrosis through decreased mesenchymal cell proliferation.

Acknowledgments This study was supported by a Research Project Grant from Kawasaki Medical School. We wish to thank Ms. Etsuko Yorimasa, Ms. Miki Ishihara, and Ms. Miyuki Yokohata for animal care, and Ms. Satomi Hanada, Ms. Keiko Satoh, and Ms. Yoshiko Shirakiya for help with in vitro experiments.

Disclosure All the authors have declared no competing interest.

References

1. Pastan S, Bailey J. Dialysis therapy. N Engl J Med. 1998;338:1428–37.
2. Gokal R, Mallick NP. Peritoneal dialysis. Lancet. 1999;353:823–8.
3. Williams JD, Craig KJ, Topley N, Von Ruhland C, Fallon M, Newman GR, Mackenzie RK, Williams GT. Morphologic changes in the peritoneal membrane of patients with renal disease. J Am Soc Nephrol. 2002;13:470–9.
4. Bonetti PO, Lerman LO, Lerman A. Endothelial dysfunction: a marker of atherosclerotic risk. Arterioscler Thromb Vasc Biol. 2003;23:168–75.
5. Albina JE, Mills CD, Henry WL Jr, Caldwell MD. Temporal expression of different pathways of 1-arginine metabolism in healing wounds. J Immunol. 1990;144:3877–80.
6. Lee PC, Salyapongse AN, Bragdon GA, Shears LL 2nd, Watkins SC, Edington HD, Billiar TR. Impaired wound healing and angiogenesis in eNOS-deficient mice. Am J Physiol. 1999;277:H1600–8.
7. Luo JD, Wang YY, Fu WL, Wu J, Chen AF. Gene therapy of endothelial nitric oxide synthase and manganese superoxide dismutase restores delayed wound healing in type 1 diabetic mice. Circulation. 2004;110:2484–93.
8. Tie L, Li XJ, Wang X, Channon KM, Chen AF. Endothelium-specific GTP cyclohydrolase I overexpression accelerates refractory wound healing by suppressing oxidative stress in diabetes. Am J Physiol Endocrinol Metab. 2009;296:E1423–9.
9. Sun D, Wang Y, Liu C, Zhou X, Li X, Xiao A. Effects of nitric oxide on renal interstitial fibrosis in rats with unilateral ureteral obstruction. Life Sci. 2012;90:900–9.
10. Kazakov A, Hall R, Jagoda P, Bachelier K, Muller-Best P, Semenov A, Lammert F, Bohm M, Laufs U. Inhibition of endothelial nitric oxide synthase induces and enhances myocardial fibrosis. Cardiovasc Res. 2013.
11. van Guldener C, Janssen MJ, Lambert J, Steyn M, Donker AJ, Stehouwer CD. Endothelium-dependent vasodilatation is impaired in peritoneal dialysis patients. Nephrol Dial Transplant. 1998;13:1782–6.
12. Shesely EG, Maeda N, Kim HS, Desai KM, Krege JH, Laubach VE, Sherman PA, Sessa WC, Smithies O. Elevated blood pressures in mice lacking endothelial nitric oxide synthase. Proc Natl Acad Sci U S A. 1996;93:13176–81.
13. Miyamoto T, Tamura M, Kabashima N, Serino R, Shibata T, Furuno Y, Miyazaki M, Baba R, Sato N, Doi Y, Okazaki M, Otsuji Y. An integrin-activating peptide, PHSRN, ameliorates inhibitory effects of conventional peritoneal dialysis fluids on peritoneal wound healing. Nephrol Dial Transplant. 2010;25:1109–19.
14. Nishi Y, Satoh M, Nagasu H, Kadoya H, Ihoriya C, Kidokoro K, Sasaki T, Kashihara N. Selective estrogen receptor modulation attenuates proteinuria-induced renal tubular damage by modulating mitochondrial oxidative status. Kidney Int. 2013;83:662–73.
15. Meuten T, Hickey A, Franklin K, Grossi B, Tobias J, Newman DR, Jennings SH, Correa M, Sannes PL. WNT7B in fibroblastic foci of idiopathic pulmonary fibrosis. Respir Res. 2012;13:62.
16. Kim YD, Park CH, Kim HS, Choi SK, Rew JS, Kim DY, Koh YS, Jeung KW, Lee KH, Lee JS, Juhng SW, Lee JH. Genetic alterations of Wnt signaling pathway-associated genes in hepatocellular carcinoma. J Gastroenterol Hepatol. 2008;23:110–8.
17. Li N, Xi Y, Tinsley HN, Gurpinar E, Gary BD, Zhu B, Li Y, Chen X, Keeton AB, Abadi AH, Moyer MP, Grizzle WE, Chang WC, Clapper ML, Piazza GA. Sulindac selectively inhibits colon tumor cell growth by activating the cGMP/PKG pathway to suppress Wnt/beta-catenin signaling. Mol Cancer Ther. 2013;12:1848–59.
18. Cooke JP, Losordo DW. Nitric oxide and angiogenesis. Circulation. 2002;105:2133–5.
19. Dumont O, Loufrani L, Henrion D. Key role of the NO-pathway and matrix metalloprotease-9 in high blood flow-induced remodeling of rat resistance arteries. Arterioscler Thromb Vasc Biol. 2007;27:317–24.
20. Schaffer MR, Tantry U, Thornton FJ, Barbul A. Inhibition of nitric oxide synthesis in wounds: pharmacology and effect on accumulation of collagen in wounds in mice. Eur J Surg. 1999;165:262–7.
21. Amadeu TP, Costa AM. Nitric oxide synthesis inhibition alters rat cutaneous wound healing. J Cutan Pathol. 2006;33:465–73.
22. Singer AJ, Clark RA. Cutaneous wound healing. N Engl J Med. 1999;341:738–46.
23. Witte MB, Barbul A. General principles of wound healing. Surg Clin North Am. 1997;77:509–28.
24. Amadeu TP, Seabra AB, de Oliveira MG, Monte-Alto-Costa A. Nitric oxide donor improves healing if applied on inflammatory and proliferative phase. J Surg Res. 2008;149:84–93.
25. Powell DW, Mifflin RC, Valentich JD, Crowe SE, Saada JI, West AB. Myofibroblasts. I. Paracrine cells important in health and disease. Am J Physiol. 1999;277:C1–9.
26. Bucala R, Spiegel LA, Chesney J, Hogan M, Cerami A. Circulating fibrocytes define a new leukocyte subpopulation that mediates tissue repair. Mol Med. 1994;1:71–81.
27. Kalluri R, Neilson EG. Epithelial-mesenchymal transition and its implications for fibrosis. J Clin Invest. 2003;112:1776–84.
28. Ignarro LJ, Cirino G, Casini A, Napoli C. Nitric oxide as a signaling molecule in the vascular system: an overview. J Cardiovasc Pharmacol. 1999;34:879–86.
29. Pyriochou A, Beis D, Koika V, Potytarchou C, Papadimitriou E, Zhou Z, Papapetropoulos A. Soluble guanylyl cyclase activation promotes angiogenesis. J Pharmacol Exp Ther. 2006;319:663–71.
30. Kotzki S, Roustit M, Arnaud C, Boutonnat J, Blaise S, Godin-Ribuot D, Cracowski JL. Anodal iontophoresis of a soluble

guanylate cyclase stimulator induces a sustained increase in skin blood flow in rats. J Pharmacol Exp Ther. 2013;346:424–31.
31. Beyer C, Reich N, Schindler SC, Akhmetshina A, Dees C, Tomcik M, Hirth-Dietrich C, von Degenfeld G, Sandner P, Distler O, Schett G, Distler JH. Stimulation of soluble guanylate cyclase reduces experimental dermal fibrosis. Ann Rheum Dis. 2012;71:1019–26.
32. Ghofrani HA, D'Armini AM, Grimminger F, Hoeper MM, Jansa P, Kim NH, Mayer E, Simonneau G, Wilkins MR, Fritsch A, Neuser D, Weimann G, Wang C. Riociguat for the treatment of chronic thromboembolic pulmonary hypertension. N Engl J Med. 2013;369:319–29.
33. Ishii Y, Sawada T, Shimizu A, Tojimbara T, Nakajima I, Fuchinoue S, Teraoka S. An experimental sclerosing encapsulating peritonitis model in mice. Nephrol Dial Transplant. 2001;16:1262–6.
34. Park SH, Kim YL, Lindholm B. Experimental encapsulating peritoneal sclerosis models: pathogenesis and treatment. Perit Dial Int. 2008;28(Suppl 5):S21–8.
35. Hung KY, Huang JW, Chiang CK, Tsai TJ. Preservation of peritoneal morphology and function by pentoxifylline in a rat model of peritoneal dialysis: molecular studies. Nephrol Dial Transplant. 2008;23:3831–40.
36. Pletinck A, Vanholder R, Veys N, Van Biesen W. Protecting the peritoneal membrane: factors beyond peritoneal dialysis solutions. Nat Rev Nephrol. 2012;8:542–50.
37. Krediet RT, Zweers MM, van der Wal AC, Struijk DG. Neoangiogenesis in the peritoneal membrane. Perit Dial Int. 2000;20(Suppl 2):S19–25.
38. Sherif AM, Nakayama M, Maruyama Y, Yoshida H, Yamamoto H, Yokoyama K, Kawakami M. Quantitative assessment of the peritoneal vessel density and vasculopathy in CAPD patients. Nephrol Dial Transplant. 2006;21:1675–81.
39. Margetts PJ, Bonniaud P. Basic mechanisms and clinical implications of peritoneal fibrosis. Perit Dial Int. 2003;23:530–41.